Progress Report 1998:
Nucleation and Breakout of Large Earthquakes

L. Knopoff

Institute of Geophysics and Planetary Physics
University of California, Los Angeles

The work outlined in our 1998 proposal has resulted in completion of a Ph.D. thesis by Dr. Xiao-xi Ni. We have embarked in a new direction concerned with generation of 3-D models of fracture in order to continue our studies of Nucleation and Breakout, and the development of other products that will result from this new research initiative. This report summarizes the new work.

The recent noteworthy success of finite difference techniques in solving dynamic fracture problems in three-dimensional environments, and especially for generating source-time functions for strong-motion applications (Olsen, et al., 1997; Madariaga, et al., 1998), have prompted us to reopen the long-standing debate about the relative merits of finite difference (FD) versus Boundary Integral or Green's function (BI) schemes to solve these difficult problems. We have a special interest in studying inhomogeneous fractures. The two approaches to fracture problems date back to the late 1960's. Both methods were applied to 1-D, and 2-D antiplane and in-plane, dynamical fracture problems, but all were severely limited by the failure of the physics to describe adequately wave propagation in the elastic medium adjacent to cracks of finite size; the difficulties are geometrical in origin. The FD models were easily applied to inhomogeneous fractures, while the BI solutions were more easily applied to homogeneous systems; Chatterjee and Knopoff (1982, 1983) extended the 2-D BI antiplane problem to inhomogeneous cracks, but the solution is not simple.

Because of the inadequacy of 1-D and 2-D models, attention has turned to the 3-D problems which are those of the fracture, healing and energy loss through elastic wave radiation, of 2-D cracks imbedded in a 3-D medium. We have developed a BI method for the solution of 3-D inhomogeneous crack problems, which has obvious and significant advantages of computational speed over FD schemes. The problem of synthesizing the influence of Rayleigh waves on the rupture history falls out naturally in our BI formulation, whereas they are awkward to develop computationally in FD versions, or if the Green's function is not carefully selected in other BI approaches to 3-D fractures (Fukuyama and Madariaga, 1995, 1998). We use the BI formulation of Das (1980) for homogeneous 3-D cracks and introduce slip-weakening into the formulation (Andrews, 1985). Our contribution is to extend this work to inhomogeneous fractures. A standard solution to the wave equation involves the convolution of a Green's function with the stress drop. We use the half-space Green's function (see Das, 1980), which is the solution to Lamb's problem for a point source in 3-D; Richards (1979) has given useful solutions to the problem. For subsonic cracks, we solve for the stresses in advance of the crack by evaluation of certain convolution integrals. The comparison of these stresses with the fracture criterion at each unfractured point determines whether the crack grows. The fracture thresholds and the stress drops can be inhomogeneous. The singularities at the edge of the crack are ameliorated by slip weakening in a zone, up to a critical slip distance Δ_0; for larger slips, the material is considered to be in the free-fracture state. Healing occurs either when the slip velocity drops to zero or to some finite, positive value.

We bypass the singularities in the Green's function associated with the Rayleigh wave by averaging across each element of the space-time integration, and further gain speed by using the FFT to calculate the convolutions of the stress drops with the Green's functions that are the heart of the computation. We speed up the calculation significantly by solving for the slip history only and defer the calculation of the motion at distance from the fault, the latter being of course the signal needed for strong motion calculations. We use a slip weakening fracture criterion, and initiate fracture in a localized zone of nucleation by applying a uniform stress in excess of the fracture threshold to it over its entire area at t=0. In the examples, the pre-fracture shear stress is uniform in the x-direction, the elastic moduli are homogeneous over the 3-D volume, the P-wave velocity is set equal to 1, and the computational grid spacing is set equal to 1.

The symmetry of the Green's function precludes the consideration of free surfaces or other non-coplanar inhomogeneities. We have sacrificed asymmetry in the interest of increased computational speed. The computation takes about 15 minutes for 60 time steps on a region 128×128 on a Sparc Ultra II workstation at 50% CPU sharing; the memory demands are 74MB. Even this speed is not practical for numerous experiments for testing assumptions, or other explorations that require many repetitions with different parameter values. For the latter purposes, and especially to explore fundamental issues of the physics of earthquakes, we continue to use 2-D antiplane (BI) dynamical fracture models, or 2-D in-plane (FD) dynamical fracture models, the latter with scaling difficulties normal to the fault. The programming was begun before the discovery (Knopoff and Landoni, 1998) that the slip-weakening fracture condition was non-causal; the weakening condition will be modified when the remedy to the causality problem will be made.

Results I: Nucleation and Breakout

We offer two examples from the application of the present version of our computer code. Both applications deal with cracks that are initially at a subcritical stress state.

We consider a subcritical crack with a prestress and fracture strength indicated in the Table. Fracture is initiated in a nucleation zone of radius R at t=0. Initially, slip and velocity build up gradually in the nucleation zone. After some time, breakout may occur if the stresses generated in the nucleation zone are large enough to overcome the subcriticality. If the system were perfectly linear, the crack properties should scale only with the ratio R/Δ_0, where R is the radius of the nucleation circle. Thus cracks with the same value of R/Δ_0 should have the same properties independent of the specific values of R or Δ_0, all values of stresses being kept constant. Under the assumption of linearity the crack should breakout from the nucleation zone for sufficiently large values of R/Δ_0. The Table lists the fracture thresholds, σ_{cri}, stress drops σ_0, and stress in excess of the threshold in the nucleation zone $\Delta\sigma$. Distances are measured in units of the computational grid size. The results show that the assumption of scaling (linearity) is not justified. For small breakout slip threshold Δ_0, the cracks break out to long distance in the region outside the nucleation zone. For larger values of Δ_0 the crack breaks for a short distance but the fracture cannot be sustained, and for large values of Δ_0, the crack never grows outside the nucleation zone. The variation in growth style is associated with both the subcriticality of all cracks, even though they are homogeneous, and the nonlinearity of the problem. The larger the value of Δ_0 the less likely the crack will break out of the nucleation zone; the scaling must take the stresses into account through the slope of the weakening function.

Results II: Detailed Rupture History

We consider an application of the program to illustrate tunneling and healing. In Fig. 1, we consider rupture in an elongated region. The long dimension is broken into three segments; the two outer subregions are square and the central region is a barrier that is half the width of the outer ones. The central barrier and the outer rectangular boundary are unbreakable;

σ_{cri}	σ_0	$\Delta\sigma$	Δ_0	R_{cri}	State
0.85	0.70	0.01	0.25	1	Breakout
0.85	0.70	0.01	0.50	2	Breakout
0.85	0.70	0.01	1.00	3	Partial Healing
0.85	0.70	0.01	2.00	4	No Initiation

elastic stress waves can propagate through the unbreakable boundaries and beyond. Both the left and right regions are homogeneous and subcritical. A fracture nucleates on a circle by elevation of the stress to slightly above the critical value at t=0. We show snapshots at intervals Δt=5 from t=0 to t=55. The two upper rows are contoured slip velocities and the two lower rows are contoured cumulative slip up to time t. From t=0 to t=10 (all times approximate) the slip and velocity in the nucleation zone increase as the material becomes weaker; at t=10 the fracture breaks out of the nucleation circle. The crack now begins to grow with P-wave velocity in the x-direction and with S-wave velocity in the y-direction, thus producing a fracture that is elongated in the x-direction. At t=20, the crack has reached the unbreakable barriers at the left boundary and the left edge of the central barrier; the profile of the crack edge begins to flatten. At t=25, the crack has reached the upper and lower boundaries. Almost the entire left square region is slipping at times t=25 and 30. Between t=30 and 35, healing begins in the left region and proceeds from the outer edges of the left subregion inward; a curiosity that we have not yet understood is the fact that healing in the y-direction is faster in the x-directions (see t=35), producing a contracting fracture that is again elongated in the x-direction. At this time (t=35), the elastic waves have tunneled through the central barrier and trigger slip in the right square; while the fracture in the left square continues to contract, the fracture in the right square expands. By t=45, the left square is no longer slipping and the cumulative slip in this region is unchanged thereafter. At t=55 the slip in the right square has not reached the level in the left square; the slip in the entire region at t=55 is plotted in Fig. 1b.

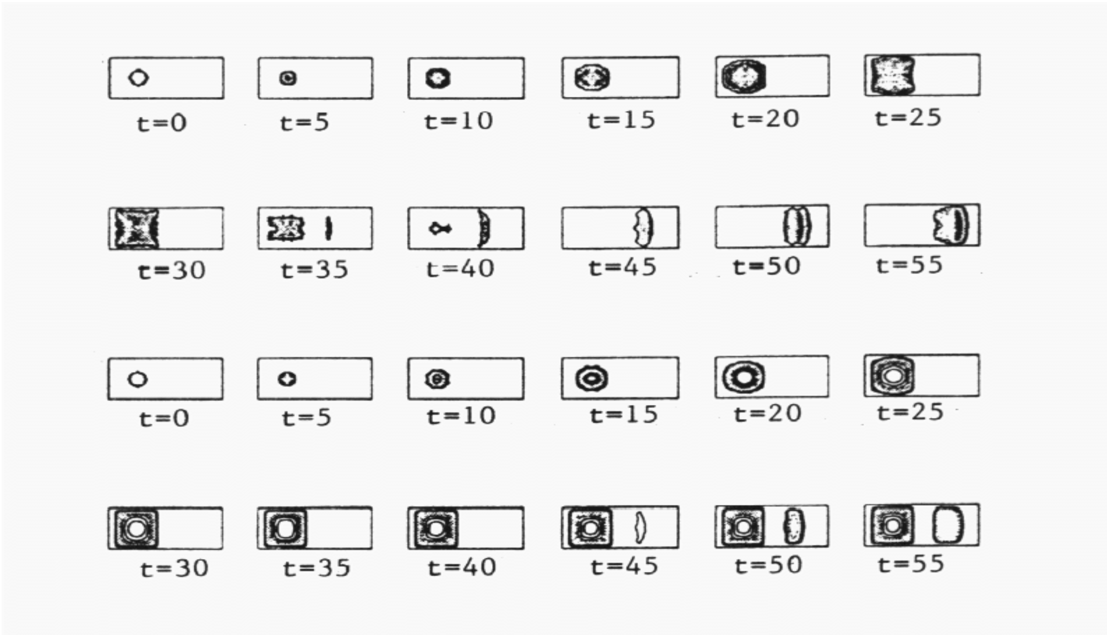

Figure 1: Rupture history of a planar fracture embedded in a 3-D elastic medium. The crack nucleates in the left subregion and, after a time delay for passage of elastic waves, it tunnels through an unbreakable barrier into the right subregion. Healing progresses inward from the outer edges of the fractured region. The upper pair of strips shows slip velocity at time intervals $\Delta t = 5$; the lower pair of strips shows cumulative slip.

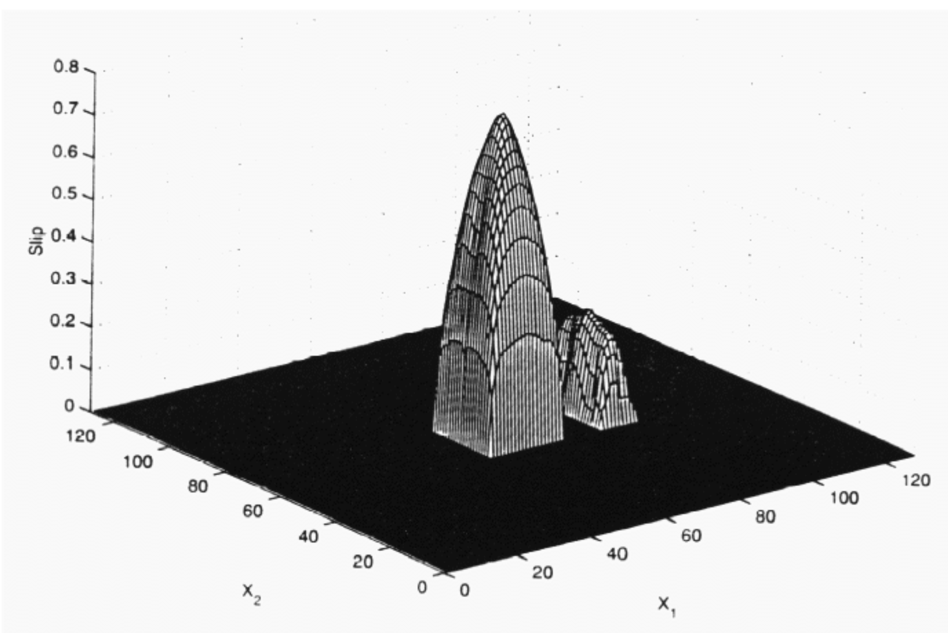

Figure 2: Cumulative slip at $t = 55$. The slip in the left subregion of the fracture plane is much larger than the slip in the right subregion. The no-slip barrier between the two regions is easily identified.

References

D.J. Andrews, Dynamic plane-strain shear rupture with a slip-weakening friction law calculated by a boundary integral method, Bull. Seismol. Soc. Amer., **75**, 1-21, 1985.

A.K. Chatterjee and L. Knopoff, Unilateral extension of a two-dimensional shear crack under the influence of cohesive forces, Geophys. J. Roy. Astron. Soc., **68**, 7-25, 1982.

A.K. Chatterjee and L. Knopoff, Bilateral propagation of a spontaneous two-dimensional anti-plane shear crack under the influence of cohesion, Geophys. J. Roy. Astron. Soc., **73**, 449-473, 1983.

S. Das, A numerical method for determination of source time functions for general three-dimensional rupture propagation, Geophys. J. Roy. Astron. Soc., **62**, 591-604, 1980.

E. Fukuyama and R. Madariaga, Integral equation method for plane crack with arbitrary shape in 3D elastic medium, Bull. Seismol. Soc. Amer., **85**, 614-628, 1995.

E. Fukuyama and R. Madariaga, Rupture dynamics of a planar fault in a 3D elastic medium: Rate- and slip-weakening function, Bull. Seismol. Soc. Amer., **88**, 1-17, 1998.

L. Knopoff and J.A. Landoni, Noncausality of fractures with linear strength-weakening, submitted, Geophys. Res. Lett., 1998.

R. Madariaga, K.B. Olsen., and R. Archuleta, Modeling dynamic rupture in a 3D earthquake fault model. Bull. Seismol. Soc. Amer., **88**, 1182-1197, 1998.

K.B. Olsen, R. Madariaga, and R.J. Archuleta, Three-dimensional dynamic simulation of the 1992 Landers earthquake, Science. **278**, 834-838, 1997.

P.G. Richards, Dynamic motions near an earthquake fault: A three-dimensional solution, Bull. Seismol. Soc. Amer., **66**, 1-32, 1976.